Energy & Environmental Science

Supporting Information

A highly tailored gap-like structure for excellent thermoelectric performance

Xiao Xu[1,#], Yi Huang[1,#], Xixi Liu[1,#], Baohai Jia[1], Juan Cui[1], Ran He[2], Jinghan Wang[1], Yiyuan Luo[1], Kornelius Nielsch[2] and Jiaqing He[1,*]

[1]Department of physics, Southern University of Science and Technology, Shenzhen, 518055, China.

[2]Institute for Metallic Materials, IFW-Dresden, Dresden, 01069, Germany.

[#]These authors contributed equally

*Correspondence: he.jq@sustech.edu.cn

Contents

Figures

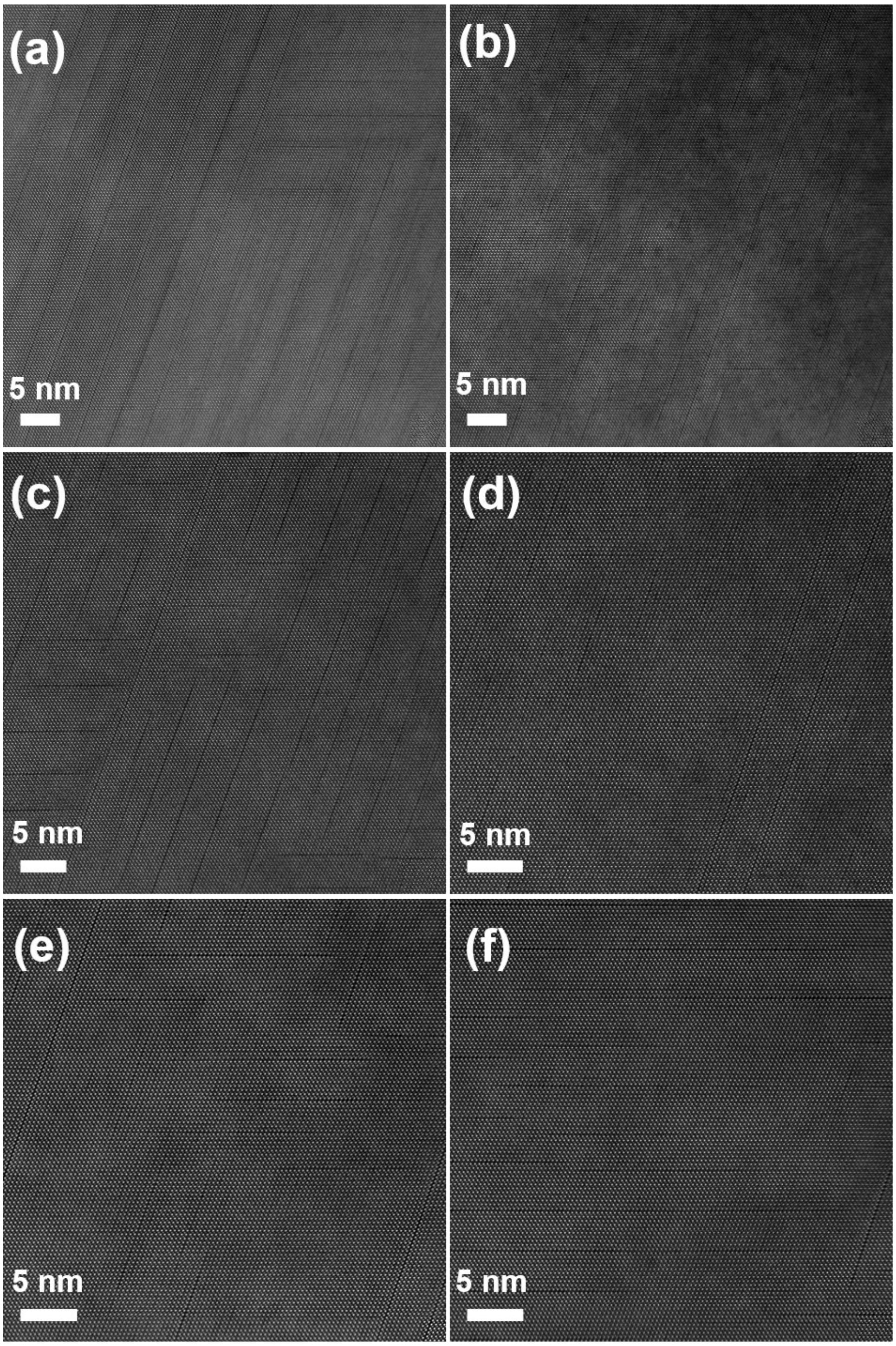

Figure S1. The high magnified STEM-HAADF images of $Sb_2Te_3(GeTe)_9$ sample.

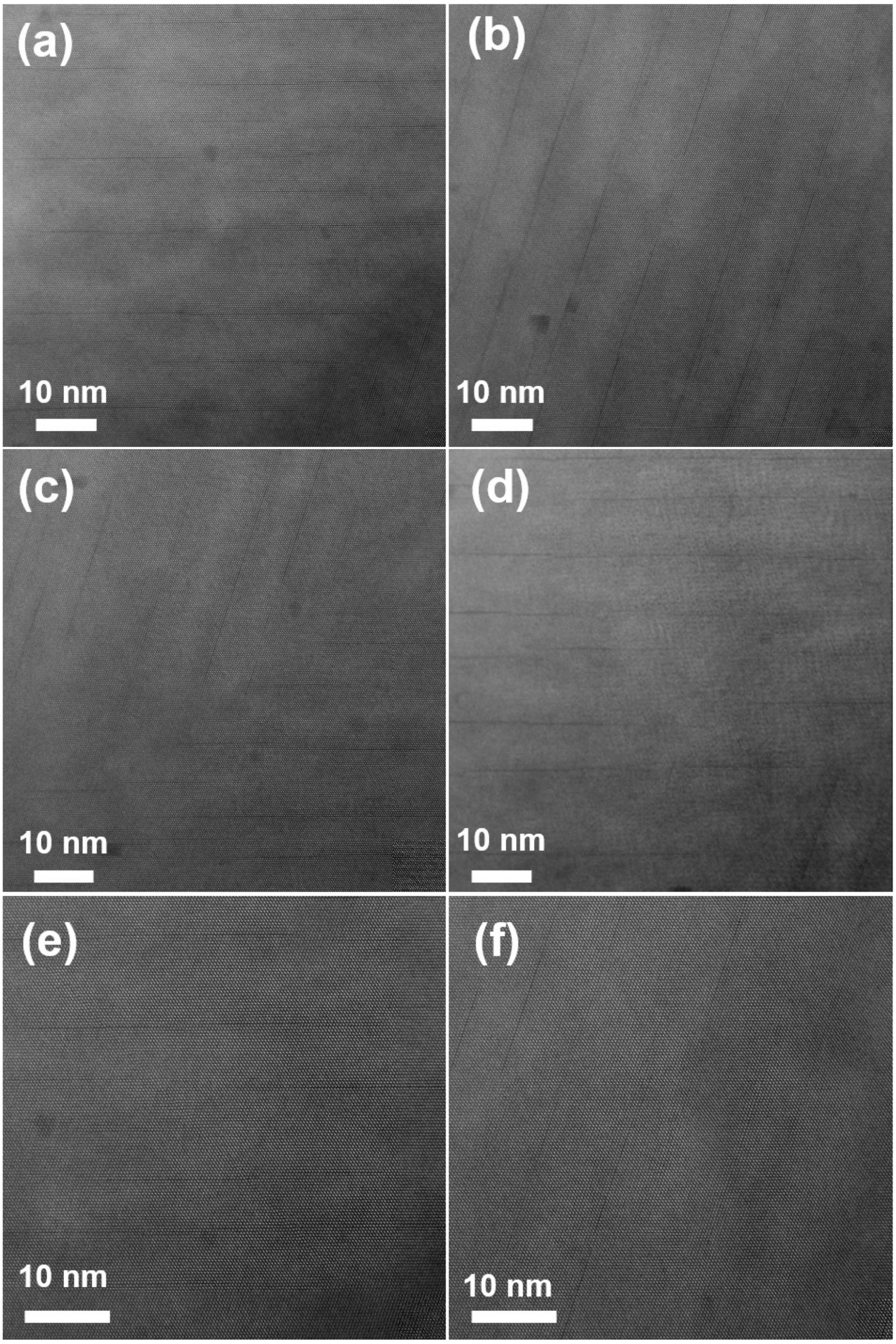

Figure S2. The high magnified STEM-HAADF images of $Sb_2Te_3(GeTe)_{17}$ sample.

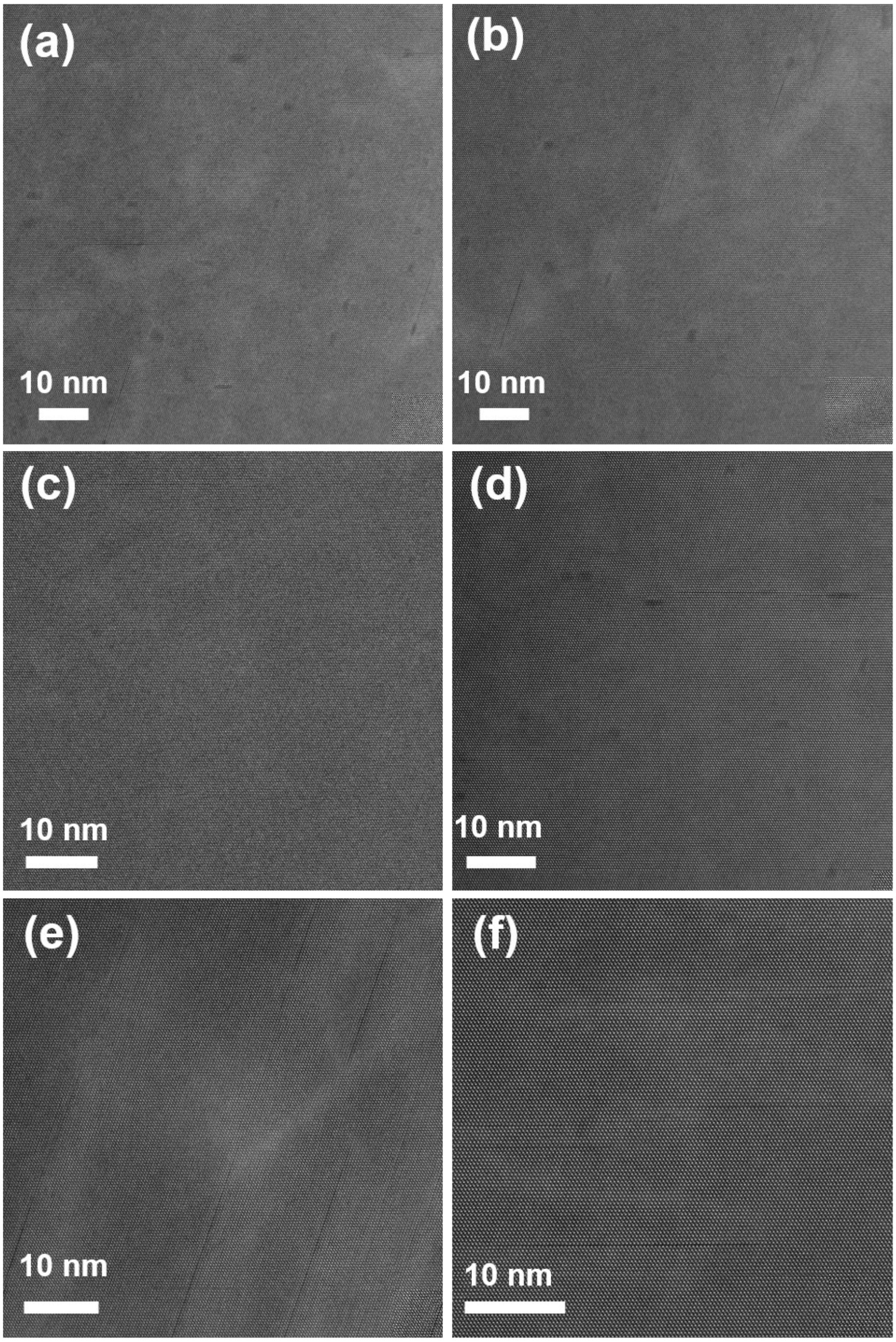

Figure S3. The high magnified STEM-HAADF images of $Sb_2Te_3(GeTe)_{34}$ sample.

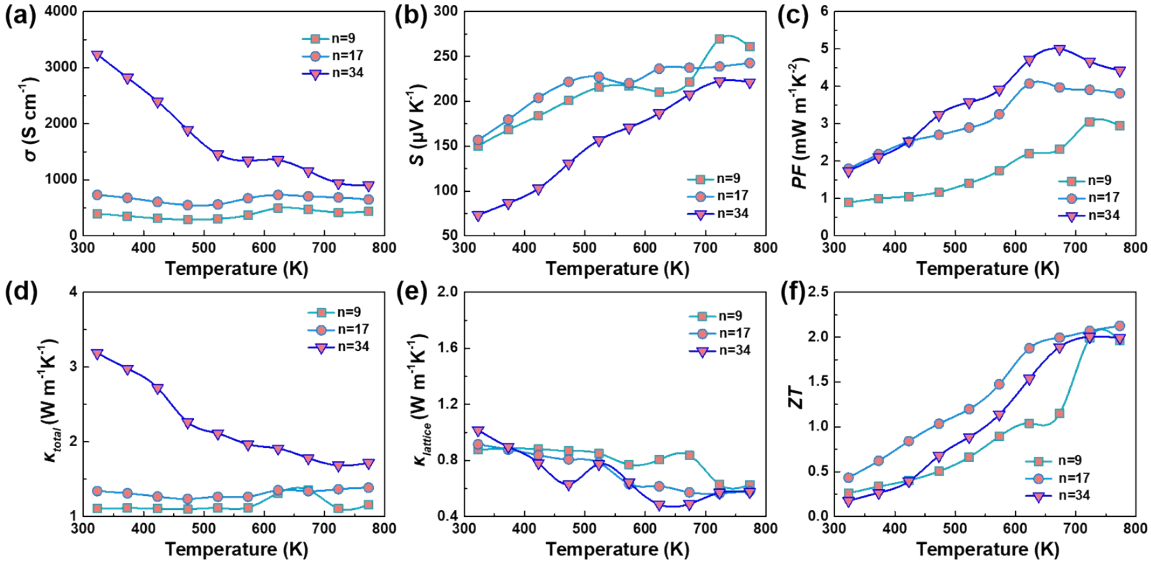

Figure S4. The temperature dependence of (a) electrical conductivity, (b) Seebeck coefficient, (c) power factor, (d) total thermal conductivity, (e) lattice thermal conductivity, and (f) *ZT* value of $Sb_2Te_3(GeTe)_n$, n equal to 9, 17, and 34, respectively.

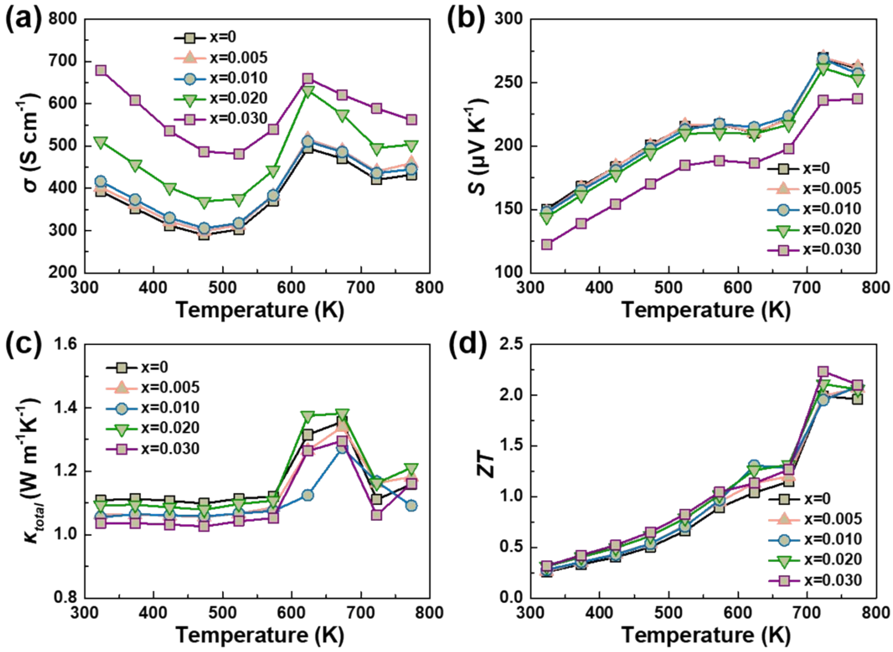

Figure S5. The temperature dependence of (a) electrical conductivity, (b) Seebeck coefficient, (c) power factor, and (d) *ZT* value of $Sb_2Te_3(Ge_{1-x}Yb_xTe)_9$.

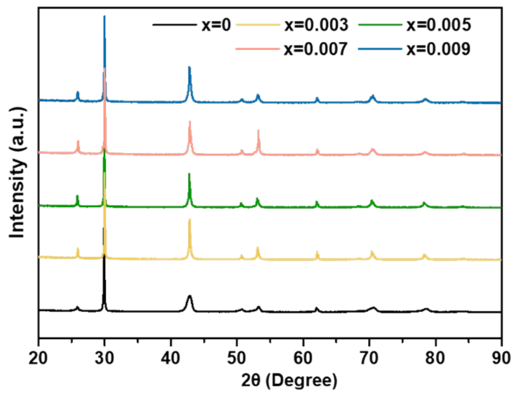

Figure S6. The XRD pattern of $Sb_2Te_3(Ge_{1-x}Yb_xTe)_{17}$ samples.

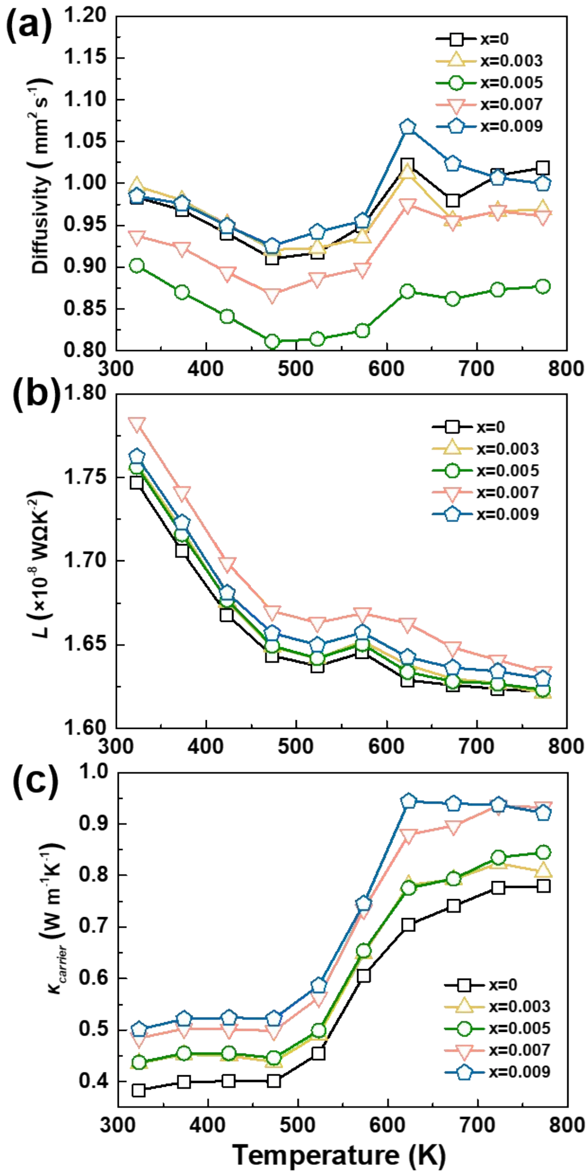

Figure S7. The temperature dependence of (a) diffusivity, (b) Lorenz number, and (c) carrier thermal conductivity of $Sb_2Te_3(Ge_{1-x}Yb_xTe)_{17}$

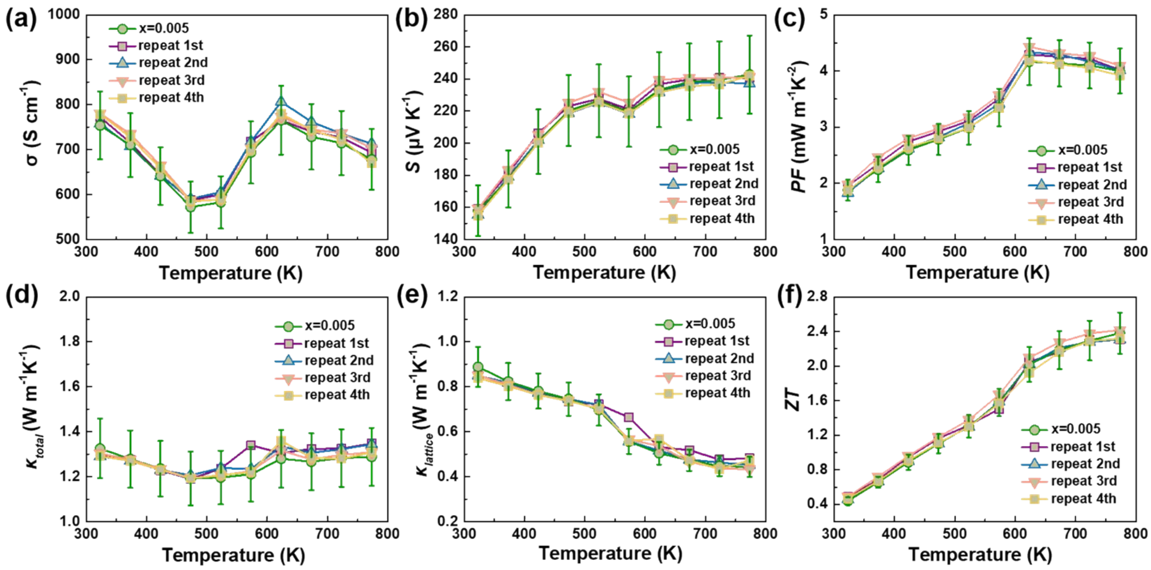

Figure S8. The repeatability test of $Sb_2Te_3(Ge_{0.995}Yb_{0.005}Te)_{17}$ sample. The temperature dependence of (a) electrical conductivity, (b) Seebeck coefficient, (c) power factor, (d) total thermal conductivity, (e) lattice thermal conductivity, and (f) *ZT* value.

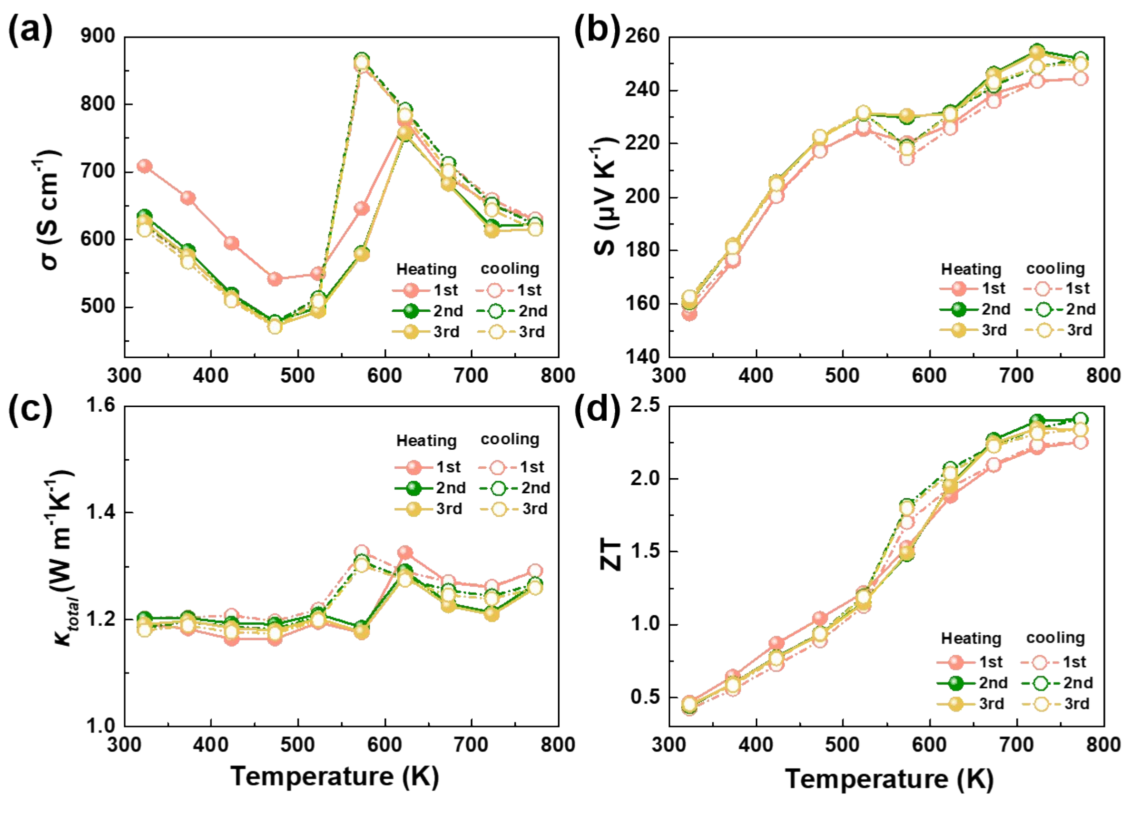

Figure S9. The cycle test of $Sb_2Te_3(Ge_{0.995}Yb_{0.005}Te)_{17}$ sample. The temperature dependence of (a) electrical conductivity, (b) Seebeck coefficient, (c) total thermal conductivity, and (d) *ZT* value.

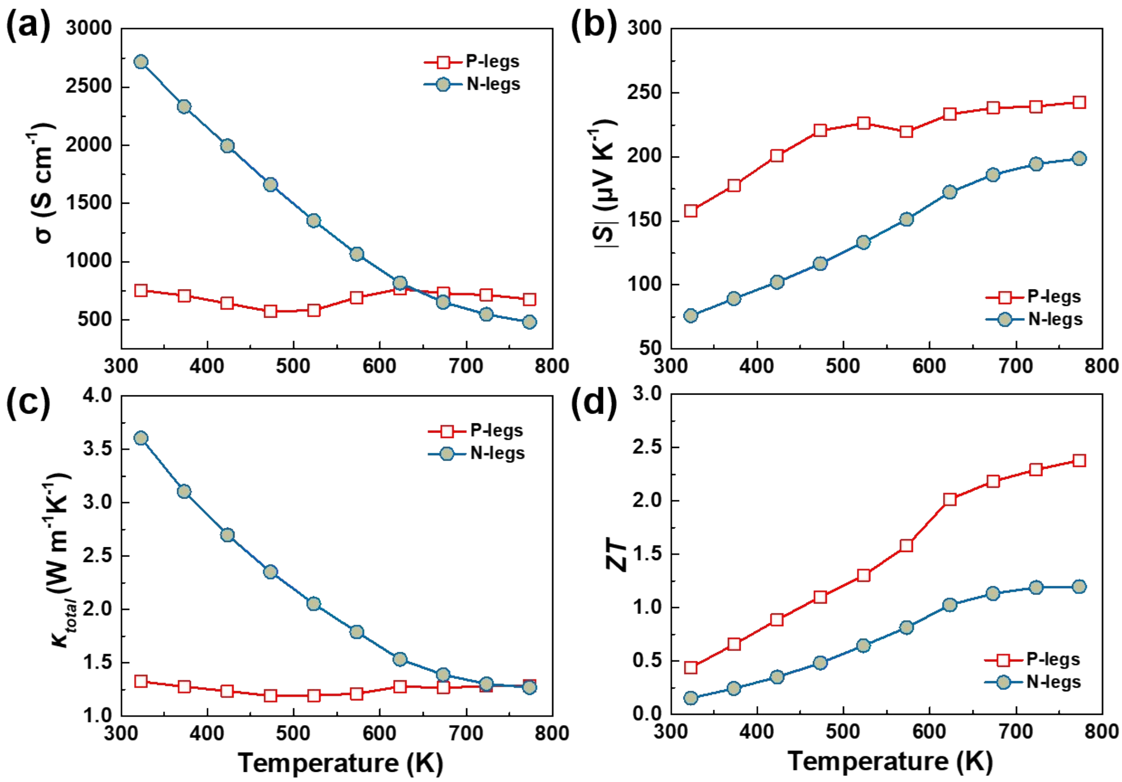

Figure S10. The temperature dependence of (a) electrical conductivity, (b) Seebeck coefficient, (c) total thermal conductivity, and (d) *ZT* value of p- and n-type leg materials.

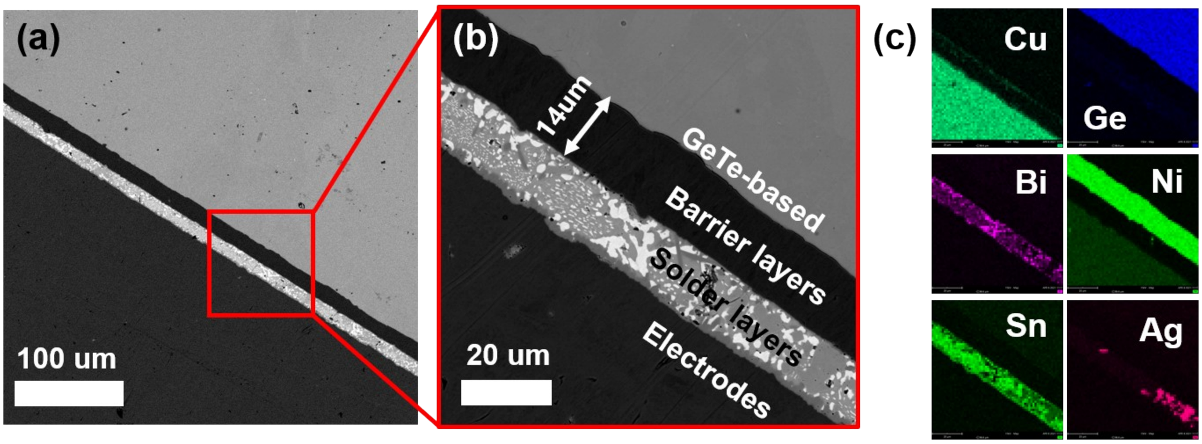

Figure S11. (a) The low magnitude SEM image and (b) the selected area SEM image of the p-type joint. (c) The EDS mapping of the corresponding area.

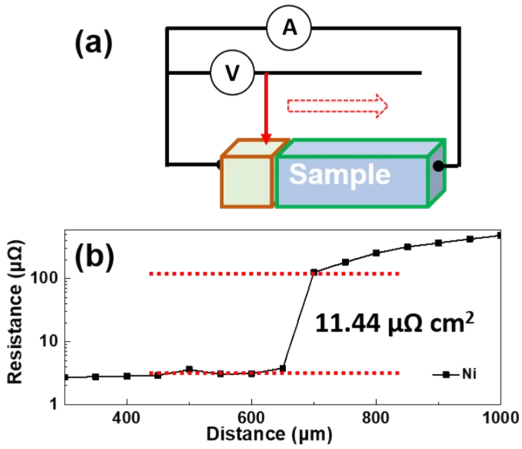

Figure S12. (a) The scheme of four probe method and (b) the resistance of p-type joint interfaces tested by four probe method.

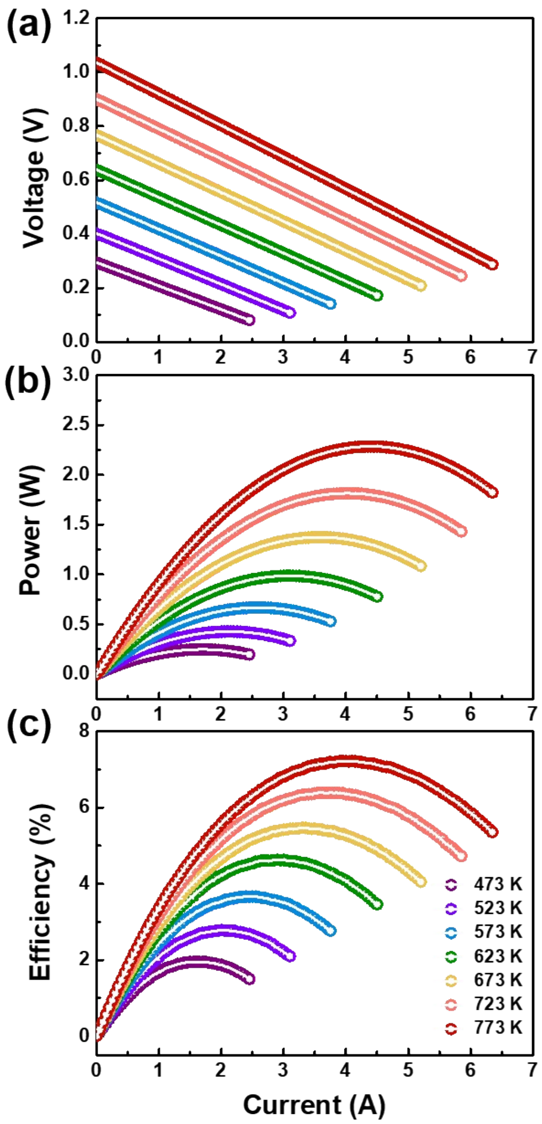

Figure S13. The current dependent (a) voltage, (b)power, and (c) efficiency of another module.

Calculation of Debye-Callaway model

To understand the phonon scattering mechanisms in this $Sb_2Te_3(GeTe)_9$ system, theoretical calculation based on the modified Callaway's model is carried out. According to Callaway's model, the lattice thermal conductivity is expressed as [1,2]:

$$\kappa_{lat} = \frac{k_B}{2\pi^2 \upsilon_{avg}} (\frac{k_B T}{\hbar})^3 \int_0^{\theta_D/T} \frac{x^4 e^x}{\tau_C^{-1}(e^x - 1)^2} dx \qquad \text{Equation (S1)}$$

where $x = \hbar\omega/k_B T$ is the reduced phonon frequency, w is the phonon frequency, k_B is the Boltzmann constant, $\hbar$ is the reduced Planck constant, w_D is the Debye temperature, and τ_C is the overall phonon scattering relaxation time. Normally, there are several scattering mechanisms can be considered. When only considering the point defect scattering (τ_{PD}), the contributions due to mass and strain contrasts are token into account. For the $Sb_2Te_3(Ge_{1-x}Yb_xTe)_9$ sample, thr ratio of κ_{lat} with disorder to that without disorder (κ_{lat0}) can be defined in terms of the scattering parameter (Γ)as,

$$\frac{\kappa_{lat}}{\kappa_{lat0}} = \frac{\tan^{-1}(\mu)}{\mu} \qquad \text{Equation (S2)}$$

$$\mu^2 = \frac{\pi^2 \Omega \theta_D}{h {\nu_s}^2} \kappa_{lat0} \Gamma \qquad \text{Equation (S3)}$$

Where μ, Ω, and ν_s are the disorder scaling parameter, the average volume per atom and the average sound velocity, respectively. As Γ can be calculated as Γ_M plus Γ_S due to mass and strain fluctuations. Then, considering Yb doped $Sb_2Te_3(Ge_{1-x}Yb_xTe)_9$, Γ can be calculated as,

$$\Gamma_{(Ge,Yb)} = \frac{9}{23} x(1 - x)[(\Delta M/M_{(Ge,Yb)})^2 + \varepsilon(\Delta\delta/\delta_{(Ge,Yb)})^2] \qquad \text{Equation (S4)}$$

$$\varepsilon = \frac{2}{9}[\frac{6.4\gamma(1 + V_p)}{1 - V_p}]^2 \qquad \text{Equation (S5)}$$

Here $M_{(Ge,Yb)}$ is the average mass of the (Ge, Yb) sites and δ is the radius of atoms of $Sb_2Te_3(Ge_{1-x}Yb_xTe)_9$ samples. V_p is the Poisson's ratio[3] and γ is the Grüneisen parameter[4].

The required physical parameters are shown in Table S1.

Calculation of Lorenz number

On the basis of single parabolic band (SPB) model, the Lorenz number can be further calculated from the following equations[5,6]:

$$S = \pm \frac{k_B}{e}\left(\frac{\left(\lambda + \frac{5}{2}\right)F_{\lambda + \frac{3}{2}}(\eta)}{\left(\lambda + \frac{3}{2}\right)F_{\lambda + \frac{1}{2}}(\eta)} - \eta\right)$$

Equation (S6)

$$F_n(\eta) = \int_0^{\infty} \frac{x^n}{1 + e^{x-\eta}}dx$$

Equation (S7)

$$L = \left(\frac{k_B}{e}\right)^2\left\{\frac{\left(\lambda + \frac{7}{2}\right)F_{r + \frac{5}{2}}(\eta)}{\left(\lambda + \frac{3}{2}\right)F_{r + \frac{1}{2}}(\eta)} - \left[\frac{\left(\lambda + \frac{5}{2}\right)F_{r + \frac{3}{2}}(\eta)}{\left(\lambda + \frac{3}{2}\right)F_{r + \frac{1}{2}}(\eta)}\right]^2\right\}$$

Equation (S8)

where λ is the scattering parameter which equals -0.5 for acoustic phonon scattering, $F_n(\eta)$ is the n-th order Fermi integral and η is the reduced Fermi energy, which can be calculated from the experimental S values.

Table S1. Physical properties used to calculate κ_{lat}

Parameters	**Values**
Debye temperature θ_D (K)	155[3]
Longitudinal sound velocity υ_L(ms^{-1})	3573[3]
Transverse sound velocity υ_T (ms^{-1})	1730[3]
Sound velocity υ(ms^{-1})	1944[3]
Poisson's ratio V_p	0.24[3]
Grüneisen parameter γ	2.19[4]
The average lattice parameter a_{lat} (Å)	6.02

Table S2. Mass densities ρ(g/cm^3) of all samples

Compositions	**ρ(g/cm^3)**	**Compositions**	**ρ(g/cm^3)**
$Sb_2Te_3(GeTe)_9$	6.2507	$Sb_2Te_3(Ge_{0.97}Yb_{0.03Te})_9$	6.2895
$Sb_2Te_3(GeTe)_{17}$	6.2243	$Sb_2Te_3(Ge_{0.997}Yb_{0.003Te})_{17}$	6.1937
$Sb_2Te_3(GeTe)_{34}$	6.2041	$Sb_2Te_3(Ge_{0.995}Yb_{0.005Te})_{17}$	6.1927
$Sb_2Te_3(Ge_{0.995}Yb_{0.005Te})_9$	6.2437	$Sb_2Te_3(Ge_{0.993}Yb_{0.007Te})_{17}$	6.2065
$Sb_2Te_3(Ge_{0.99}Yb_{0.01Te})_9$	6.2453	$Sb_2Te_3(Ge_{0.991}Yb_{0.009Te})_{17}$	6.1959
$Sb_2Te_3(Ge_{0.98}Yb_{0.02Te})_9$	6.2686		

References

1. J. Callaway, *Phys. Rev.* 1959, **113**, 1046.
2. B. Abeles, *Phys. Rev.* 1963, **131**, 1906.
3. Y. Gelbstein, J. Davidow, E. Leshem, O. Pinshow, S. Moisa, *Phys. Status Solidi B* 2014, **251**, 1431.
4. J. Li, Y. Xie, C. Zhang, K. Ma, F. Liu, W. Ao, Y. Li, C. Zhang, *ACS Appl. Mater. Inter.* 2019, **11**, 20064.
5. M. Zhou, Z. Gibbs, H. Wang, Y. Han, C. Xin, L. Li, G. Snyder, *Phys. Chem. Chem. Phys.* 2014, **16**, 20741.
6. G. Tan, F. Shi, J. Doak, H. Sun, L. Zhao, P. Wang, C. Uher, C. Wolverton, V. Dravid, M. Kanatzidis, *Energy Environ. Sci.* 2015, **8**, 267.